Magnetic Resonance Imaging 55 (2019) 103–111

Contents lists available at ScienceDirect

Magnetic Resonance Imaging

journal homepage: www.elsevier.com/locate/mri

Original contribution

A histogram analysis of diffusion and perfusion features of cervical cancer based on intravoxel incoherent motion magnetic resonance imaging

Deepa Thapa[a,1], Panying Wang[a,b,1], Guangyao Wu[a,b,*], Xiangyu Wang[a], Qunqi Sun[c]

[a] Department of Radiology, Zhongnan Hospital of Wuhan University, Wuhan 430071, PR China
[b] Department of Radiology, Shenzhen University General Hospital and Shenzhen University Clinical Medical Academy, Shenzhen 518060, PR China
[c] Department of Radiology, Yuebei People's Hospital affiliated to Shantou University Medical College, Shaoguan, 512026, PR China

ARTICLE INFO

Keywords:
Cervical cancer
Gluteus maximus
Myometrium
Intravoxel incoherent motion magnetic resonance imaging
Diffusion-weighted imaging

ABSTRACT

Objective: To evaluate the diagnostic potential based on histogram analysis of IVIM parameters between uterine cervical cancers (CC) - normal myometrium (Myo) versus CC - gluteus maximus muscle (GM) and to study the feasibility of histogram analysis of IVIM parameters to differentiate the early from locally advanced stage CCs.
Methods: 64 patients with pathologically confirmed CC were enrolled. Histogram indices mean, median, 25th, and ð 75th percentile of apparent diffusion coefficient (ADC), true diffusion coefficient (D), pseudo-diffusion coefficient (D*), and perfusion fraction (*f*) value of entire tumor were statistically analyzed and compared between CC - GM versus CC - Myo, as well as between early and locally advanced stage CCs. A multivariate analysis was performed to identify indices that could best distinguish early from locally advanced stage CC. Receiver operating characteristic curves (ROC) were used to evaluate the diagnostic efficiency of every histogram parameter.
Results: All the tested histogram indices significantly differed between the patients with CC - GM vs. CC - Myo, nonetheless, CC - GM yielded higher range area under the curve (AUC) value of 0.8–0.99 vs. 0.6–0.99. The additional significant difference was found among all the tested histogram indices of D*, mean, median, and 75th percentile of *f*, mean and 75th percentile of ADC, and 75th percentile of D discriminating early from locally advanced CCs. ROC curves indicated that the 75th percentile of D* value 28.17×10^{-3} mm^2/s could best differentiate early from locally advanced stage CCs, with AUC of 0.776. In the multivariate analysis, ROC indicated the 50th percentile of D* and *f* was the most significant with AUCs of 0.856.
Conclusions: The histogram analysis of IVIM parameters depicted that gluteus maximus served better reference tissue in comparison to myometrium. The histogram index 75th percentile of ADC, D, D*, and *f* may serve a diagnostic biomarker to differentiate the early from locally advanced stage CCs.

1. Introduction

Cervical cancer is one of the second most common cancer worldwide and from the recent cancer statistics, it is reported to be the fourth leading cause of cancer death in women whereas in developing countries this malignancy still tops the list [1, 2]. The correct diagnosis and appropriate staging of the cervical tumor are the most important areas for accurate management. The detection of an abnormal uterine cervical tissue by conventional MRI is limited to the anatomical information lacking functional information, while diffusion-weighted imaging characterizes tissue cellularity by evaluating diffusion of water molecules for better differentiation between benign and malignant lesions [3]. Several studies have postulated that ADC value of CC is lower than normal cervical tissue [4, 5] however, there is considerable overlap in ADC values of benign and malignant tumors.

Recently, biexponential model, Intravoxel Incoherent Motion Diffusion-Weighted Imaging model is being increasingly used in the study of gynecological problems. Unlike the monoexponential model, IVIM-MRI involves multiple b values, where lower b values (< 200 s/mm^2) are sensitive to capillary perfusion and higher b values (> 200 s/mm^2) contributes to the true water diffusion [6]. Studies have suggested that DW images with high b values are affected by noise effect, long acquisition and the depth of the tissue so to overcome these disadvantages more stable but similar type of tissue can be studied. Previous studies have demonstrated that malignant tissue yield lower diffusion and perfusion characteristics than normal tissue [7, 8], however,

* Corresponding author at: Department of Radiology, Zhongnan Hospital of Wuhan University, Wuhan 430071, PR China.
E-mail address: wuguangy2002@163.com (G. Wu).
[1] Deepa Thapa and Panying Wang contributed equally to this work.

https://doi.org/10.1016/j.mri.2018.06.016
Received 30 May 2018; Received in revised form 22 June 2018; Accepted 24 June 2018

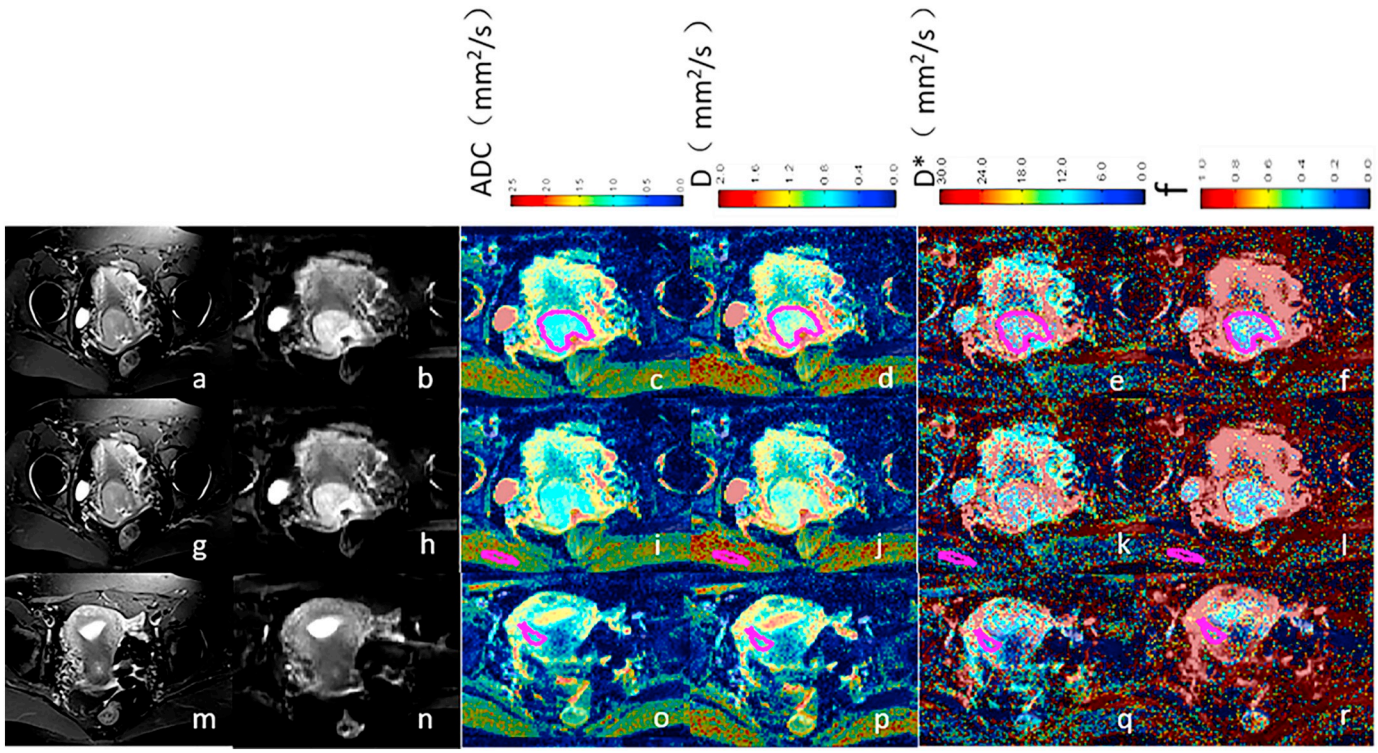

Fig. 1. A 44 -year-old patient with cervical squamous cell carcinoma clinical stage II_B (a–f), gluteus maximus muscle (g–l), and normal myometrium (m–r). Outlines indicate the tumor area and tested tissue areas respectively. (a, g, m) Axial T2-weighted images. (b, h, n) Axial DW images. (c, i, o) Axial ADC maps. (d, j, p) Axial D map. (e, k, q) D* map. (f, l, r) *f* map values. Values obtained for cervical cancer, gluteus maximus muscle and normal myometrium were as follows: ADC: 1.01×10^{-3} mm²/s, 1.37×10^{-3} mm²/s, and 1.08×10^{-3} mm²/s; D: 0.93×10^{-3} mm²/s, 1.28×10^{-3} mm²/s, 0.97×10^{-3} mm²/s; D*: 21.14×10^{-3} mm²/s, 19.25×10^{-3} mm²/s, and 25.16×10^{-3} mm²/s; and *f*: 0.09, 0.18, and 0.20, respectively.

Table 1
Baseline information of the patients with clinical stages and pathological classification.

Characteristics	Cases (*n*)
No of patients	64
Patient age (mean ± SD, range)	52.20 ± 11.60 (24–81 y)
Pathology	
Squamous cell carcinomas	64
FIGO stage	
IB	12
IIA	12
IIB	29
III	9
IV	2

Table 2
Measure of reproducibility of D, D*, f and also ADC values with respective histogram indices.

Parameters	ICC (95% confidence interval, 95% CI)
ADC ($\times 10^{-3}$ mm²/s)	
Mean	0.91% (88.7%–93.1%)
25th percentile	0.90% (87.7%–91.1%)
50th percentile	0.93% (89.7%–95.2%)
75th percentile	0.90% (88.1%–91.9%)
D ($\times 10^{-3}$ mm²/s)	
Mean	93.4% (89.7%–95.1%)
25th percentile	91.1% (89.7%–93.1%)
50th percentile	91.0% (88.7%–93.1%)
75th percentile	90.1% (87.7%–92.1%)
D* ($\times 10^{-3}$ mm²/s)	
Mean	66.8% (64.7%–67.1%)
25th percentile	67.7% (66.7%–68.8%)
50th percentile	65.1% (63.7%–66.9%)
75th percentile	66.7% (64.7%–68.1%)
f (%)	
Mean	82.5% (81.7%–83.1%)
25th percentile	80.2% (78.7%–83.1%)
50th percentile	77.1% (76.7%–78.1%)
75th percentile	73.4% (70.7%–74.5%)

no comparative studies have been done so far between CC - GM vs. CC - Myo to find out which one among GM and Myo serves better reference tissue. This article aimed to compare the diagnostic efficacy between CC - GM tissue vs. CC - Myo tissues using quantitative histogram analysis of IVIM parameters and to study the feasibility of IVIM parameters using quantitative histogram analysis to differentiate the early stage from locally advanced stage CCs.

2. Materials and methods

2.1. Patient population

This retrospective study was conducted in a single center over a period of 3 years (June 2014–2017), where pathologically proven patients were included. Informed consent was obtained from all the participants. A total of 64 early and locally advanced stage cervical lesions, 58 myometrial tissues and 64 gluteus maximus tissues were included in the study. According to the 2009 International Federation of Gynecologists and Obstetricians (FIGO) staging system and histopathology results, the clinical staging were as follows: I_B = 12 patients, II_A = 12 patients, II_B = 29 patients, III = 9 patients, IV = 2 patients. They were further divided into early stage (I_B - II_A, n = 24) and locally advanced stage (II_B - IV, n = 40) CCs. The inclusion criteria for the patient selection had the ensuing conditions: (a) patients were not subjected to relevant treatment before MRI examination and no MRI contraindications were present; (b) pathological results were obtained via hysterectomy and/or Pap smear.

2.2. Imaging acquisition

The MRI scans were performed on a 1.5 T whole-body scanner (GE Medical System, Milwaukee, WI, USA) using 8-channel phased array torso coil with parallel imaging (acceleration factor = 2). The DWI acquisition of IVIM data used single-shot spin-echo echo-planar imaging with 11 b-values (0, 20, 30, 50, 80, 100, 150, 200, 500, 800 and 1000 smm^2). The other imaging parameters were as follows: repetition time (TR) = 4000 ms, echo time (TE) = 78.6 ms, flip angle = 90°, the number of signal averages (NSA) = 4, field of view (FOV) = 320 mm^2, slice thickness = 5.5 mm, number of slice = 20, scanning time = 4mins and 30 s, spacing between slices = 6.5 mm.

2.3. Image analysis

To obtain the IVIM parameters (D, D*, and *f*), we applied the model proposed by Le Bihan:

$$S_{(b)}/S_{(0)} = f \times e^{-b \cdot D*} + (1 - f) \times e^{-b(D+D*)}$$

where $S_{(b)}$ and S_0 represent the signal intensity of the corresponding voxel at the given b values and at b = 0 s/mm^2 respectively. D is true diffusion coefficient, D* is the pseudo diffusion coefficient, and *f* is the

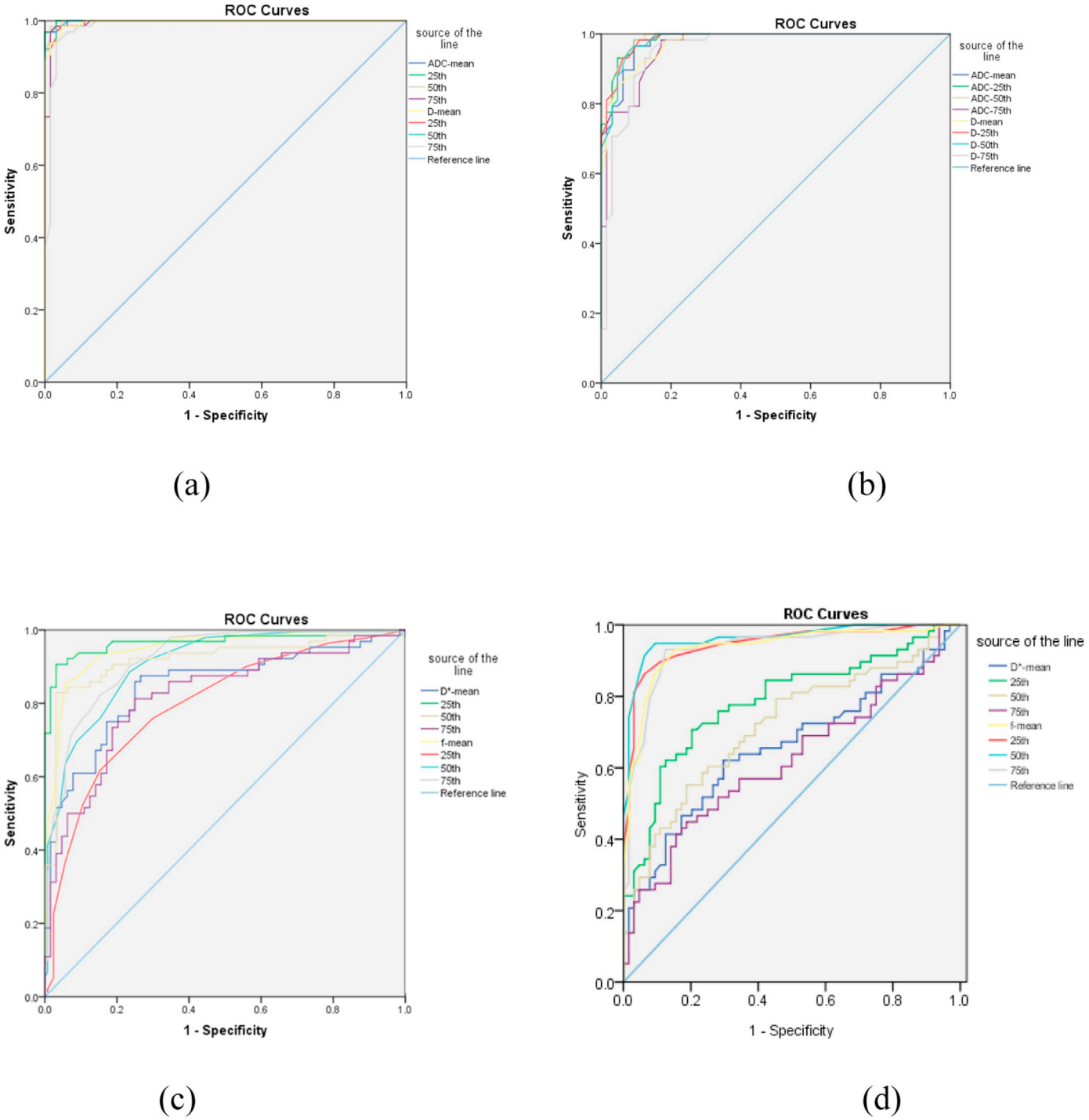

Fig. 2. (a) and (b) are ROC curves of the mean, median, 25th, and 75th percentile of ADC and D values and (c) and (d) are ROC curves of mean, median, 25th, and 75th percentile of D* and *f* values comparing cervical cancer and gluteus maximus versus cervical cancer and myometrium.

perfusion fraction.

All data analyses were post-processed using the in-house software written in MATLAB 2013 (Mathworks, MA, USA). The ADC map was obtained from the same software using a simple monoexponential fit on a voxel-by-voxel basis with all b-values, as shown below:

$$S(b)/S(0) = \exp(-b \times ADC)$$

Two expert radiologists, who were blinded to the information of patients, together reviewed the MRI images and quantitatively analyzed the IVIM images. They reviewed the IVIM sequences and drew region of interest (ROI) around the tumor, the visually necrotic and cystic lesions were excluded from the ROI, and all the slices in which the tumors were included were used for the ROI delineation polygonal ROI. The ROIs were also placed in the gluteus maximus and normal myometrium avoiding bleeding, myoma, and uterine adenomyosis. Those patients with cervical lesions encroaching the myometrium and uterine atrophy were excluded. ROIs from the CC, GM, and normal Myo were calculated with all b-values using the in-house software. The quantitative histogram analysis, mean, median, 25th, and 75th percentile pixel values of ADC, D, D*, and *f* histograms were obtained and recorded from the entire tumor volume, gluteus maximus, and myometrium. Subsequently, the IVIM parametric maps, namely D, *f*, and D* maps, were generated (Fig. 1). T1-weighted images and T2-weighted images were used as references.

2.4. Statistical analysis

SPSS for Windows (v.21.0; SPSS, Chicago, IL, USA) was used for data analysis. Quantitative variables were compared using Student's *t*-test or Mann-Whitney *U* test as appropriate. The performance of each parameter was evaluated using the ROC analysis and the AUC, obtained from MatLab. AUC value was calculated to ascertain the diagnostic accuracy. The optimal sensitivity and specificity values were selected at the point on the ROC curve analysis. The ROC analysis identified the diagnostic ability of each parameter in discriminating CC - GM vs. CC - Myo and also for distinguishing the early and locally advanced stages for CCs. In addition, multivariate analysis was used to identify diagnostic factor for early and locally advanced stage CCs. The cut-off value for significant parameters were established by calculating the maximal Youden index (Youden index = sensitivity + specificity-1). *P* - values < 0.05 were considered significant.

3. Results

The presence of squamous cell carcinoma of the uterine cervix in all 64 patients confirmed via pathology was enrolled in this retrospective study. This study had extracted normal myometrial tissues from only 58 patients because the cervical lesions encroaching the myometrium with a large amount of effusion ($n = 2$) and uterine atrophy ($n = 4$) were excluded. The final cohort consisted of 64 patients with FIGO stage I_B - IV CCs (age 52.2 ± 11.6; range 24–81 years), gluteus maximus tissue from 64 patients and myometrial tissue from 58 patients. Thus, ROIs consisted of 64 CCs, 64 GM and 58 normal Myo. The baseline information of the patients with clinical stages and pathological classification was presented in Table 1.

3.1. IVIM parameters in cervical cancer - gluteus maximus versus cervical cancer - myometrium

All the tested histogram parameters mean, median, 25th, and 75th percentile of ADC, D, D*, and *f* demonstrated a significant difference for CC-GM vs. CC-Myo with *P* values (< 0.001 vs. < 0.001–0.021) (Table 2). ROC curve analysis of these significant parameters demonstrated powerful discrimination between the compared two groups (Fig. 2). All the tested histogram parameters, mean, median, 25th, and 75th percentile of ADC, D, D*, and mean *f* demonstrated significant differences for CC - GM except median, 25th, and 75th percentile of *f*, which were slightly higher in CC - Myo. The AUC values, sensitivity, and specificity values of these histogram parameters at optimal cut-off values are shown in Table 3 and Table 4.

3.2. IVIM parameters in early and advanced stage cervical cancer

Regarding the early and locally advanced stages of CC, mean, median, 25th, and 75th percentile of D*, mean, median, and 75th percentile of *f*, mean and 75th percentile of ADC, and 75th percentile of D ($P \leq 0.001$, $P = 0.002$, $P \leq 0.001$, $P \leq 0.001$, $P = 0.004$, $P = 0.012$, $P = 0.006$, $P = 0.021$, $P = 0.012$, $P = 0.035$ respectively) showed significant discrimination between early and locally advanced stage CCs (Table 5, Fig. 3). The 75th percentile was the common histogram index for ADC, D, D*, and *f* that significantly differed in all tested parameters ($P = 0.012$, $P = 0.035$, $P \leq 0.001$ and $P = 0.006$ respectively) (Fig. 4). The ROC curve and optimal cut-off values of these significant parameters showed unsurpassed discrimination between early and advanced stage CCs. The 75th percentile of D* was the most robust parameter, with AUC of 0.776. (Table 6 and Fig. 5).

3.3. Multivariate analyses with significant IVIM parameters

Multivariate analyses were obtained by adding significant

Table 3
Comparison of ADC and IVIM - histogram parameters between two groups, cervical cancer - myometrium and cervical cancer - gluteus maximus.

Parameters		Cervical cancer ($n = 64$)	Myometrium ($n = 58$)	Gluteus maximus ($n = 64$)	*P* value (CC-Myo)	*P* value (CC-GM)
ADC ($\times 10^{-3}$ mm^2/s)	mean	0.94 ± 0.13	1.32 ± 0.15	1.40 ± 0.10	< 0.001	< 0.001
	25th	0.80 ± 0.12	1.23 ± 0.15	1.30 ± 0.09	< 0.001	< 0.001
	50th	0.89 ± 0.13	1.32 ± 0.15	1.39 ± 0.10	< 0.001	< 0.001
	75th	1.02 ± 0.16	1.41 ± 0.16	1.48 ± 0.10	< 0.001	< 0.001
D ($\times 10^{-3}$ mm^2/s)	mean	0.84 ± 0.11	1.17 ± 0.16	1.24 ± 0.11	< 0.001	< 0.001
	25th	0.72 ± 0.11	1.06 ± 0.13	1.12 ± 0.11	< 0.001	< 0.001
	50th	0.80 ± 0.12	1.15 ± 0.13	1.24 ± 0.10	< 0.001	< 0.001
	75th	0.92 ± 0.15	1.25 ± 0.13	1.35 ± 0.11	< 0.001	< 0.001
D* ($\times 10^{-3}$ mm^2/s)	mean	23.08 ± 5.51	26.96 ± 7.55	16.44 ± 3.91	0.002	< 0.001
	25th	7.99 ± 2.33	11.85 ± 4.51	3.82 ± 0.95	< 0.001	< 0.001
	50th	14.85 ± 5.70	21.00 ± 8.60	7.61 ± 2.28	< 0.001	< 0.001
	75th	32.06 ± 10.3	37.02 ± 13.04	20.15 ± 8.18	0.021	< 0.001
f (%)	mean	0.14 ± 0.03*	0.24 ± 0.06	0.23 ± 0.04	< 0.001	< 0.001
	25th	0.09 ± 0.03	0.19 ± 0.06	0.12 ± 0.03	< 0.001	< 0.001
	50th	0.13 ± 0.03*	0.24 ± 0.06	0.19 ± 0.04	< 0.001	< 0.001
	75th	0.18 ± 0.04*	0.30 ± 0.08	0.27 ± 0.05	< 0.001	< 0.001

* = test was done using Mann-Whitney *U* test.

Table 4
ROC analysis of apparent diffusion coefficient and IVIM histogram parameters for cervical cancer - myometrium.

Parameters		AUC	Cut off value	Sensitivity	Specificity
ADC ($\times 10^{-3}$ mm^2/s)	mean	0.980	1.12	0.966	0.906
	25th	0.986	0.97	0.983	0.906
	50th	0.98s6	1.07	0.983	0.906
	75th	0.964	1.19	0.983	0.828
D ($\times 10^{-3}$ mm^2/s)	mean	0.973	0.98	0.914	0.891
	25th	0.986	0.85	0.983	0.891
	50th	0.983	0.94	0.966	0.906
	75th	0.954	1.05	0.966	0.844
D* ($\times 10^{-3}$ mm^2/s)	mean	0.657	25.35	0.621	0.703
	25th	0.786	9.43	0.707	0.797
	50th	0.716	18.60	0.552	0.812
	75th	0.619	41.04	0.431	0.828
f (%)	mean	0.936	0.17	0.931	0.844
	25th	0.947	0.13	0.862	0.937
	50th	0.963	0.17	0.948	0.906
	75th	0.935	0.23	0.931	0.875

Table 5
ROC analysis of apparent diffusion coefficient (ADC) and IVIM histogram parameters for cervical cancer-gluteus maximus.

Parameters		AUC	Cut off value	Sensitivity	Specificity
ADC ($\times$10–^{3} mm^2/s)	mean	0.998	1.24	0.969	1
	25th	0.999	1.07	1	0.969
	50th	0.998	1.20	0.984	0.984
	75th	0.994	1.30	0.984	0.969
D ($\times$10–^{3} mm^2/s)	mean	0.996	1.02	0.984	0.953
	25th	0.996	0.90	0.984	0.953
	50th	0.997	1.05	0.984	0.969
	75th	0.985	1.17	0.969	0.938
D* ($\times$ 10–^{3} mm^2/s)	mean	0.845	18.50	0.875	0.734
	25th	0.965	5.76	0.906	0.969
	50th	0.919	10.81	0.828	0.969
	75th	0.818	24.21	0.813	0.750
f (%)	mean	0.947	0.20	0.859	0.938
	25th	0.802	0.10	0.766	0.703
	50th	0.908	0.15	0.891	0.766
	75th	0.920	0.22	0.828	0.844

parameters, 75th percentile of ADC and D, mean and 75th percentile of ADC and D*, mean and 75th percentile of ADC and *f*, 75th percentile of D and D*, mean and 75th percentile of D and *f*, median and 75th percentile of D* and *f* to identify the independent diagnostic parameter for early and advanced stage CCs. The ROC curve analyses obtained adding D* and *f* demonstrated the most robust discrimination between early and locally advanced stage CCs (Fig. 6). The AUC values of 50th and 75th percentile are 0.856 and 0.848 with a sensitivity of 88% and 80% and specificity of 79% and 83% respectively (Table 7). (See Table 8.)

4. Discussion

The results of our study showed the diagnostic potential of histogram analysis of IVIM parameters in CCs. Previous reports have stated that the ADC and IVIM parameters have successfully differentiated malignant cervical lesion from normal tissue [9–12]. To the best of our knowledge, this is the first report on such comparative application of CC-GM vs. CC-Myo. In this comparative study, the histogram parameters ADC, D, D* and mean *f* of CC-GM exhibited better discrimination than CC-Myo, only 25th, 50th, and 75th percentile of *f* showed slightly higher significance for myometrium. This could be attributed to hormonal influenced increased capillary volume during the secretory phase of uterus since some of the studied subjects were in their reproductive age group [13]. The perfusion value is also affected by other factors, such as relaxation effects and T2 contribution; myometrium with high T2 value yields high *f* and low T2 value has low *f* [13, 14]. GM is a superficial and more stable tissue compared to Myo, and our data supported that GM muscle served a better reference tissue compared to Myo in monitoring the recurrent/residual tumor post-therapy, also in patients with large cervical tumor encroaching myometrium, with a large amount of effusion and in patients with uterine atrophy and bleeding.

In this study, we selected the normal myometrium (far from CC, > 3 cm) and GM of the same patients with CC rather than the cervix or Myo of the other normal subjects for the control group. This might be ascribed to the previous IVIM study on cervical cancer, wherein the parameters between CC tissue and normal cervical tissue and normal myometrium were statistically significant, and the parametric values of normal cervix and myometrium were similar. So, the 'normal cervical

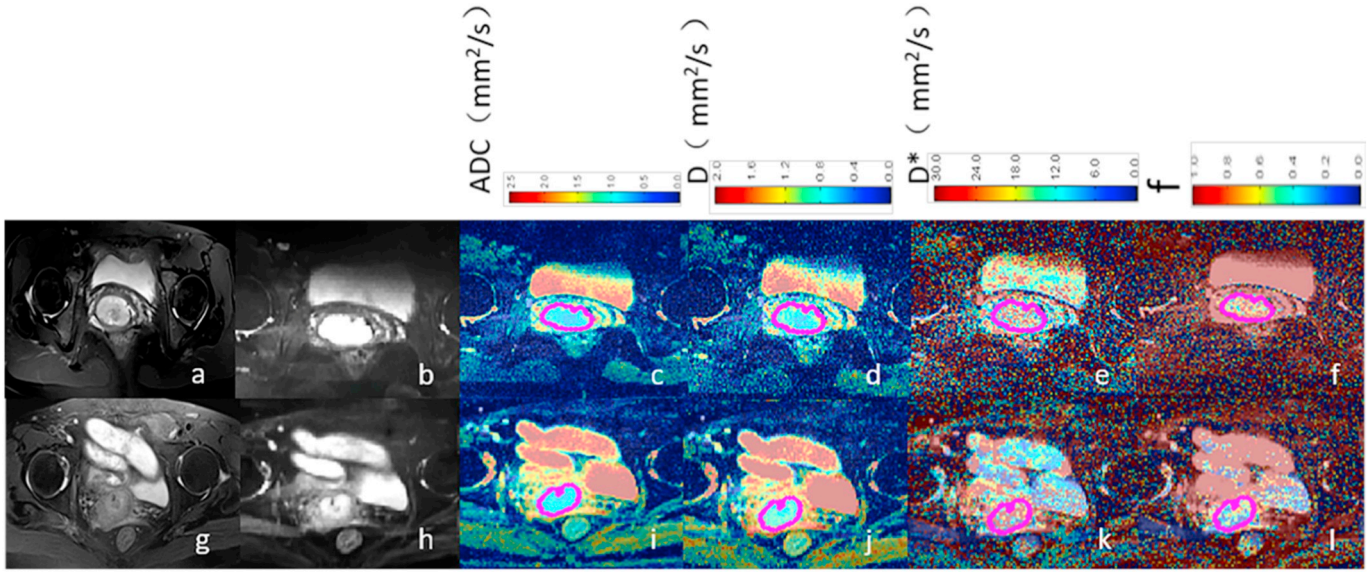

Fig. 3. A 41 years old patient with cervical squamous cell carcinoma, clinical stage I_B (a–f). Another 61 years old patient with cervical squamous cell carcinoma, clinical stage II_B (g–l). (a) Axial FS hyperintense T2-weighted image, (b, h) Axial DW images. (c, i) Axial ADC maps. (d, j) Axial D map. (e, k) D* map. (f, l) *f* map values. (g) Axial FS hypointense T2-weighted image. Values obtained for clinical stage I_B and clinical stage II_B cervical cancer were as follows: ADC: 1.10×10^{-3} mm^2/s and 0.88×10^{-3} mm^2/s; D: 1.00×10^{-3} mm^2/s and 0.85×10^{-3} mm^2/s; D*: 21.02×10^{-3} mm^2/s and 31.63×10^{-3} mm^2/s; and *f*: 0.17 and 0.11, respectively.

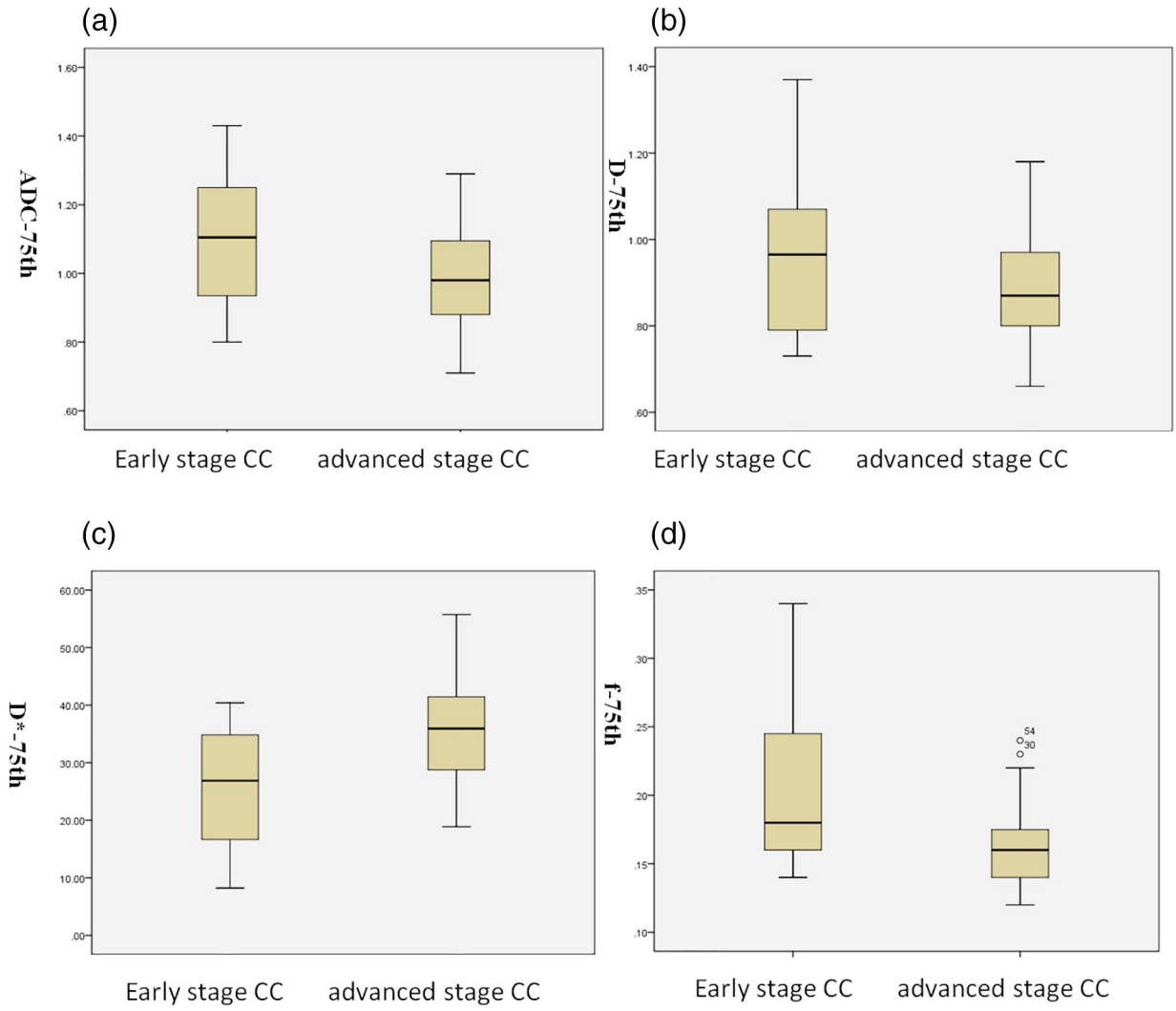

Fig. 4. Box plots (a), (b), (c), and (d) represent 75th percentile of ADC, D, D* and *f* values for early and advanced stage cervical cancer ($P = 0.012$, $P = 0.035$, $P = 0.001$ and $P = 0.006$).
Note: circles represent outliers.

standard comparison', might use their own Myo and GM that reduced the workload of the researchers and also avoided the acquired and environmental discrepancies among different individuals [15]. Our study once again emphasized factors such as tumor size, stage, and patient age may influence the homogeneity test.

Table 6
Comparison of early and advanced stage cervical cancer based on ADC and IVIM histogram parameters.

Parameters		Early stage CC (mean ± SD)	Advanced stage CC (mean ± SD)	*P* value
ADC ($\times 10^{-3}$ mm^2/s)	Mean	0.99 ± 0.15	0.91 ± 0.11	0.021
	25th	0.83 ± 0.15	0.79 ± 0.10	0.242
	50th	0.93 ± 0.17	0.86 ± 0.10	0.056
	75th	1.09 ± 0.18	0.98 ± 0.13	0.012
D ($\times 10^{-3}$ mm^2/s)	mean	0.87 ± 0.13	0.82 ± 0.10	0.100
	25th	0.73 ± 0.12	0.72 ± 0.10	0.610
	50th	0.82 ± 0.14	0.79 ± 0.10	0.242
	75th	0.97 ± 0.17	0.89 ± 0.12	0.035
D* ($\times 10^{-3}$ mm^2/s)	mean	19.73 ± 5.29	25.09 ± 4.64	< 0.001
	25th	6.83 ± 2.11	8.68 ± 2.19	0.002
	50th	11.63 ± 3.86	16.79 ± 5.79	< 0.001
	75th	25.68 ± 9.66	35.88 ± 8.85	< 0.001
f (%)	mean	0.17 ± 0.05	0.13 ± 0.02	0.004
	25th	0.10 ± 0.05	0.09 ± 0.02	0.142
	50th	0.15 ± 0.05	0.12 ± 0.02	0.012
	75th	0.20 ± 0.06	0.07 ± 0.03	0.006

Tumor biological properties may change within short periods of time, where one part may be viable and the other necrotic so mean quantitative values may not be sensitive enough to represent the precise status of the tumor [16]. Histogram analysis of tumor is a systematic approach to study the tumor heterogeneity that helps in the accurate assessment of the entire tumor that influences the diagnosis. Better staging of the heterogeneous biology of a tumor with non-invasive methods to understand tumor environment and the development of new clinically relevant biomarkers are of paramount importance. With the advent of newer imaging technique evaluation of tumor heterogeneity with histogram analysis improved enormously providing better vision into diffusion and perfusion features of tumor biology [17].

IVIM is the technique that studies both diffusion and perfusion within tumor voxel [18]. Another entity we studied was the feasibility of histogram analysis of IVIM parameters of CC into early and locally advanced stages. The present study found that histogram analyses of IVIM parameters were more advantageous over diffusion-weighted MR images with respect to clinical staging. The apparent diffusion coefficient in cervical cancer is decreased, however, its value may remain same as normal tissue in early and well/moderately differentiated malignancy [19]. Lee et al. in their study stated that parameters of IVIM

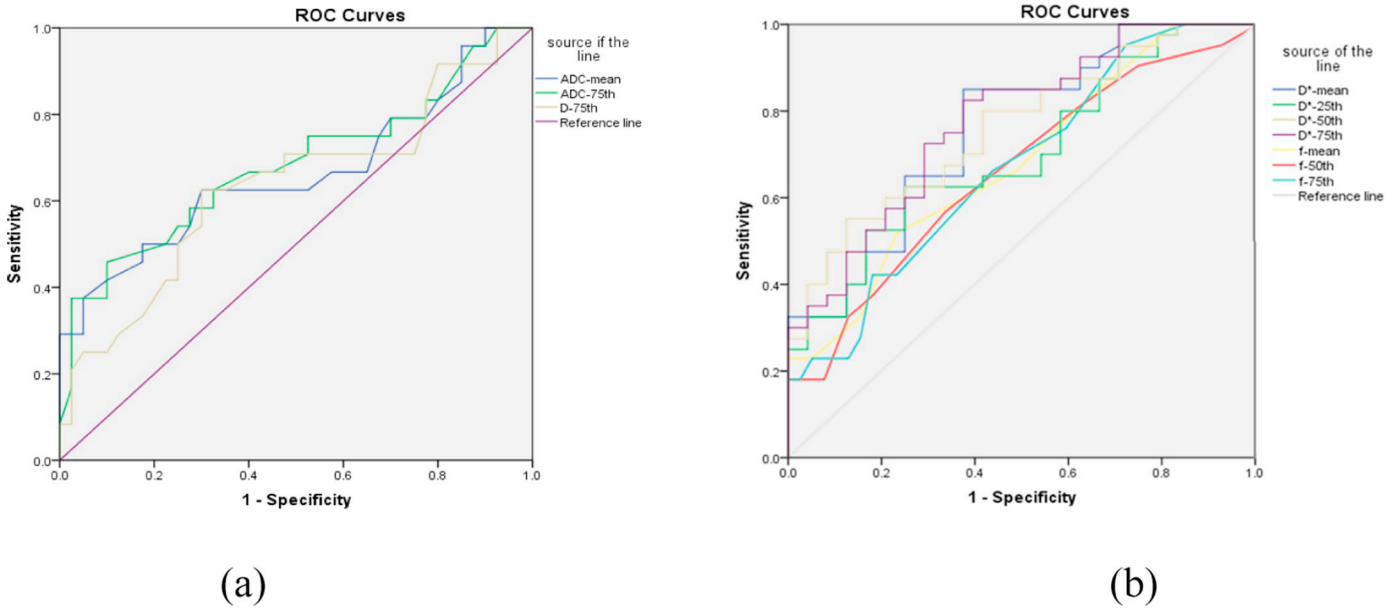

Fig. 5. ROC curve of mean and 75th percentile of ADC, 75th percentile of D, mean, 25th, 50th, and 75th percentile of D*, and mean, 50th, and 75th percentile of *f* values differentiating early from locally advanced stage cervical cancer.

showed better discrimination than ADC, demonstrating that ADC overestimated the diffusion of molecule[11]. Moreover, previous studies demonstrated that the lower ADC values in the advanced stages are mainly due to decreased perfusion rather than decreased extravascular diffusion [20]. Our study consisted of more number of locally advanced stage patients than the early stage, and interestingly, perfusion-related parameters (D* and f) also depicted more significantly different results than the diffusion related parameters.

The use of IVIM histogram analysis approach proved an innovative way to study the heterogeneous tumor than simple statistical mean values of the parameters. Mean and 75th percentile of ADC, 75th percentile of D, mean, median, 25th, and 75th percentile of D*, and mean, median, and 75th percentile of *f* showed a significant difference in differentiating early from locally advanced stage CCs. This histogram analysis revealed a significant association between the studied histogram indices, where 75th percentile was the common histogram index that was significant for all the perfusion and diffusion parameters and the 75th percentile of D* was the most robust parameter, with AUC of 0.776. According to the multivariate analysis, the 50th percentile of D* and *f* was the most robust and independent factor to discriminate the stages of CCs with AUC of 0.856, a sensitivity of 87% and specificity of 79%. Unlike the previous studies [5, 21], where the value of D* was explained to be of high uncertainty, this histogram analysis and multivariate analysis proved it otherwise. Moreover, perfusion-related

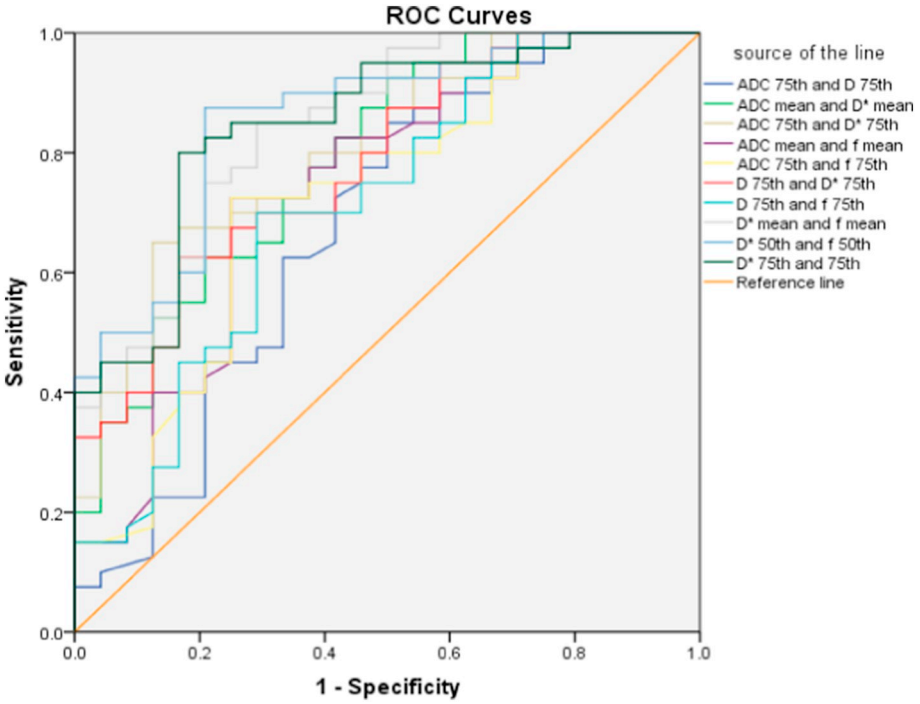

Fig. 6. ROC curves for multivariate values differentiating early from locally advanced stage cervical cancer.

Table 7
ROC analysis of significant apparent diffusion coefficient (ADC) and IVIM histogram parameters distinguishing early from advanced stage cervical cancer.

Parameters		AUC	Cut off value	Sensitivity	Specificity
ADC ($\times 10^{-3}$ mm^2/s)	mean	0.663	1.03	0.500	0.825
	75th	0.682	1.12	0.458	0.900
D ($\times 10^{-3}$ mm^2/s)	75th	0.636	0.94	0.625	0.700
D* ($\times 10^{-3}$ mm^2/s)	mean	0.759	21.06	0.850	0.625
	25th	0.700	7.89	0.625	0.750
	50th	0.759	14.77	0.550	0.875
	75th	0.776	28.17	0.825	0.625
f (%)	mean	0.716	0.15	0.583	0.750
	50th	0.697	0.17	0.292	1
	75th	0.707	0.24	0.292	0.975

Table 8
Multivariate analysis of significant parameters obtained from ROC.

Parameters		AUC	Sensitivity	Specificity
ADC and D	75th	0.680	0.850	0.500
ADC and D*	mean	0.789	0.925	0.500
	75th	0.804	0.650	0.875
ADC and *f*	mean	0.741	0.725	0.750
	75th	0.723	0.725	0.750
D and D*	75th	0.781	0.625	0.833
D and *f*	75th	0.710	0.700	0.708
D* and *f*	mean	0.846	0.850	0.708
	50th	0.856	0.875	0.792
	75th	0.848	0.800	0.833

parameters D* and *f* may be better suited to the discrimination of staging of CCs as all the histogram parameters of D* and 3 histogram parameters of *f* were highly significant than the pure molecular diffusion parameter, D. According to the double exponential theory, in tumors D* reflects the blood velocity of microcapillary and *f* demonstrates the blood volume of the microcapillary, together they display the angiogenesis and interstitial fluid pressure [13, 22]. Several studies had reported D* for data instability and the huge standard deviation and its dependence on SNR (signal-noise-ratio) [23]. We observed similar defects in our study, however, the robustness of perfusion-related parameters (D* and *f*) can neither be denied nor can be underestimated in the diagnosis and staging of the tumor. So we emphasize to make efforts to improve the SNR of this parameter in future studies. Although, our study highlighted the powerful discrimination of D* and *f*, interestingly, the 75th percentile of D and ADC were also significant histogram parameters, so all of these parameters remain important diagnostic biomarkers in the staging of CC non-invasively. The histogram analysis of IVIM method for discriminating tumor stage in our study was probably good due to improved imaging measure and which is based on entire tumor histogram analysis.

Our study has some limitations. First, unlike some previous studies [24], we did not include minimum or maximum ADCs and IVIM parameters for the histogram analysis because during the process of defining tumor region, some normal tissue with or without compression, ischemia, or edema around the tumor might be included and thus, could possibly contribute to extremely low or high parameters. Therefore, we discarded those two extreme values for the analysis. Second, with increasing age the atrophy of the gluteus maximus muscle was not considered in this study, more studies can be done in future to explore on this ground.

In conclusion, this study demonstrated the feasibility of histogram analysis of IVIM parameters in the evaluation of distinctive pattern of diffusion and perfusion characteristics of cervical cancer, myometrium, and gluteus maximus, depicting gluteus maximus to serve a better reference tissue in comparison to myometrium. And it's potential for staging the CCs into early and locally advanced stages, hence proving it's useful for tissue differentiation.

Abbreviations

IVIM	intravoxel incoherent motion
DWI	diffusion-weighted imaging
ADC	apparent diffusion coefficient
D*	pseudo-diffusion coefficient
f	perfusion fraction
D	pure diffusion coefficient
CC	cervical cancer
GM	gluteus maximus
Myo	myometrium
FIGO	International Federation of Gynecologists and Obstetricians
SNR	signal-noise-ratio
ROC	receiver operating characteristic
AUC	area under the curve
ROI	region of interest

Acknowledgement

This study was supported by national key basic research program National Natural Science Foundation of China (Grant No. 2016YFC1304702) and Major Program of the National Natural Science Foundation of China (Grant No. 81227902). We thank Dr. Fen Xin and Dr. Tu Ning from the Department of Radiology for their indispensable assistance in acquiring MR scans of patients.

Conflict of interest

All the authors declare that they do not have any conflict of interest.

Acknowledgement

We thank Dr. Fen Xin and Dr. Tu Ning from the Department of Radiology for their indispensable assistance in acquiring MR scans of patients.

References

[1] Balleyguier C, Sala E, Da Cunha T, Bergman A, Brkljacic B, Danza F. Staging of uterine cervical cancer with MRI: guidelines of the European Society of Urogenital Radiology. Eur Radiol 2011;21(5):1102–10. https://doi.org/10.1007/s00330-010-1998-x.
[2] Manoharan D, Das CJ, Aggarwal A, Gupta AK. Diffusion weighted imaging in gynecological malignancies-present and future. World J Radiol 2016;8(3):288–98. https://doi.org/10.4329/WJR.v8.i3.288.
[3] Lin Y, Li H, Chen Z, et al. Correlation of histogram analysis of apparent diffusion coefficient with uterine cervical pathologic finding. AJR Am J Roentgenol 2015;204:1125–31. https://doi.org/10.2214/AJR.14.13350.
[4] Tian T, Zhang GF, Zhang H, Liu H. Intravoxel incoherent motion diffusion-weighted imaging in differentiating uterine fibroid from focal adenomyosis: initial results. SpringerPlus 2016;9(5):1–11. https://doi.org/10.1186/s40064-015-1635-x.
[5] Wu Q, Wang Y, Shi L, Dong L, Liu M, Dou S. Intravoxel incoherent motion diffusion-weighted magnetic resonance imaging of cervical cancer with different b-values. J Comput Assist Tomogr 2017;41(4):592–8. https://doi.org/10.1097/RCT.0000000000000569.
[6] Wan Q, Deng Y, Zhou J, Yu Y, Bao Y, Lei Q. Intravoxel incoherent motion diffusion-weighted MR imaging in assessing and characterizing solitary pulmonary lesions. Nat Publ Group 2017;151:1–8. https://doi.org/10.1038/srep43257.
[7] Wang Y, Hu S, Hu X, et al. Intravoxel incoherent motion magnetic resonance imaging for diagnosis of cervical cancer and evaluation of the response of uterine cervical cancer to radio-chemotherapy: a pilot study. Oncol Transl Med 2015;1(4):164–70. https://doi.org/10.1007/s10330-015-0105-9.
[8] Koh D, Collins DJ, Orton MR. Intravoxel incoherent motion in body diffusion-weighted MRI: reality and challenges. AJR Am J Roentgenol 2011;196(6):1351–61. https://doi.org/10.2214/AJR.10.5515.
[9] Chen YB, Liao J, Xie R, Chen GL, Chen G. Discrimination of metastatic from hyperplastic pelvic lymph nodes in patients with cervical cancer by diffusion-weighted magnetic resonance imaging. Abdom Imaging 2011;36:102–9. https://doi.org/10.1007/s00261-009-9590-z.
[10] Cao K, Gao M, Sun Y, et al. Apparent diffusion coefficient of diffusion-weighted MRI

in endometrial carcinoma — relationship with local invasiveness. Eur J Radiol 2012;81:1926–30. https://doi.org/10.1016/j.ejrad.2011.04.019.
[11] Yuen E, Lee P, Yu X, Man M, Chu Y. Perfusion and diffusion characteristics of cervical cancer based on Intravoxel incoherent motion MR imaging-a pilot study. Eur Radiol 2014;24:1506–13. https://doi.org/10.1007/s00330-014-3160-7.
[12] Kilickesmez O, Bayramoglu S, Inci E, Cimilli T, Kayhan A. Quantitative diffusion-weighted magnetic resonance imaging of normal and diseased uterine zones quantitative diffusion-weighted magnetic resonance imaging of normal and diseased uterine zones. Acta Radiol 2009;50(3):340–7. https://doi.org/10.1080/02841850902735858.
[13] Liu J, Wan Y, Wang Z, Qi Y, Qu P. Perfusion and diffusion characteristics of endometrial malignancy based on intravoxel incoherent motion MRI at 3.0 T: comparison with normal endometrium. Acta Radiol 2016;57(9):1140–8. https://doi.org/10.1177/0284185115618550.
[14] Lemke A, Laun FB, Simon D, Stieltjes B, Schad LR. An in vivo verification of the intravoxel incoherent motion effect in diffusion-weighted imaging of the abdomen. Magn Reson Med 2010;64:1580–5. https://doi.org/10.1002/mrm.22565.
[15] Wang P, Thapa D, Wu G, Sun Q, Cai H, Tuo F. A study on diffusion and kurtosis features of cervical cancer based on non-Gaussian diffusion-weighted model. Magn Reson Imaging 2017;47:60–6. https://doi.org/10.1016/j.mri.2017.10.016.
[16] Just N. Improving tumor heterogeneity MRI assessment with histograms. BJC 2014;111(12):2205–13. https://doi.org/10.1038/bjc.2014.512.
[17] Huang Z, Yuh KA, Lo SS, et al. Validation of optimal DCE-MRI perfusion threshold to classify at-risk tumor imaging voxels in heterogeneous cervical cancer for outcome prediction. Magn Reson Imaging 2014;32(10):1198–205. https://doi.org/10.1016/j.mri.2014.08.039.
[18] Le Bihan D, Breton E, Lallemand D. MR imaging of intravoxel incoherent motions: application to diffusion and perfusion in neurologic disorders. Radiology 1986;161(2):401–7.
[19] Motoshima S, Irie H, Nakazono T, Kamura T, Kudo S. Diffusion-weighted MR imaging in gynecologic cancers. J Gynecol Oncol 2011;22(4):275–87.
[20] Surov A, Meyer HJ, Höhn A, et al. Correlations between intravoxel incoherent motion (IVIM) parameters and histological findings in rectal cancer: preliminary results. Oncotarget 2017;8(13):21974–83.
[21] Zhang Y, Wang Q, Wu C. The histogram analysis of diffusion-weighted intravoxel incoherent motion imaging for differentiating the Gleason grade of prostate cancer. Eur Radiol 2014. https://doi.org/10.1007/s00330-014-3511-4.
[22] Zhang B, Liang L, Dong Y, Lian Z, Chen W. Intravoxel incoherent motion MR imaging for staging of hepatic fibrosis. PLoS One 2016;1(11):1–13. https://doi.org/10.1371/journal.pone.0147789.
[23] Nougaret S, Vargas HA, Sudre R, et al. Intravoxel incoherent motion – derived histogram metrics for assessment of response after combined chemotherapy and radiation therapy in rectal cancer: initial experience and comparison between single-section. Radiology 2016;280(2):446–54.
[24] Morgan VA, Giles SL, Attygalle AD, Shepherd JH, Nandita M. Relationship between imaging biomarkers of stage I cervical cancer and poor-prognosis histologic features: quantitative histogram analysis of diffusion-weighted MR images. AJR Am J Roentgenol 2013;200:314–20. https://doi.org/10.2214/AJR.12.9545.